Modelling Amazon fire regimes under climate change scenarios

Leonardo A. Saravia [1 5], Korinna T. Allhoff [2 3], Ben Bond-Lamberty [4], Samir Suweis [5]

1. Centro Austral de Investigaciones Científicas (CADIC-CONICET), Ushuaia, Argentina.
2. University of Hohenheim, Institute of Biology, FG Eco-Evolutionary Modelling (190m), Stuttgart, Germany
3. KomBioTa – Center for Biodiversity and Integrative Taxonomy, University of Hohenheim & State Museum of Natural History, Stuttgart, Germany
4. Pacific Northwest National Laboratory, Joint Global Change Research Institute, 5825 University Research Court #3500, College Park, MD 20740, USA
5. Laboratory of Interdisciplinary Physics, Department of Physics and Astronomy "G. Galilei", University of Padova, Padova, Italy
6. Corresponding author e-mail lasaravia@untdf.edu.ar, ORCID https://orcid.org/0000-0002-7911-4398

Abstract

Fire is one of the most important disturbances of the earth-system, shaping the biodiversity of ecosystems and particularly forests. Climatic change and other anthropogenic drivers such as deforestation and land use change could produce abrupt changes in fire regimes, potentially triggering transition from forests to savannah or grasslands ecosystems with large accompanying biodiversity losses. The interplay between climate change and deforestation might intensify fire ignition and spread, potentially giving rise to more extensive, intense, and frequent fires, but this is highly uncertain. We use a simple forest-fire model to analyze the possible changes in the Amazon region's fire regime that depend on climate change-related variables. We first explored the model behavior and found that there are two possible regime changes: a critical regime that implies high variability in fire extension and mega-fires, and an absorbing phase transition which would produce the extinction of the forest and transition to a different vegetation state. We parameterize the model using remote sensing data on fire extension and temperature, and show that it demonstrates proficiency in predicting past fires. Upon considering 21st-century climate projections and deforestation scenarios, our findings suggest that the Amazon region is not currently nearing any of these regime changes but predict a consistent increase in fire extension mainly induced by deforestation. Therefore, stopping deforestation could be an important factor in reducing the potential for drastic alterations in tropical forests of the Amazon region.

Introduction

Few regions of the terrestrial biosphere are unaffected by fire. Fires caused directly or indirectly by human activities (Bowman et al. 2020) have different characteristics from natural fires, including in spatial pattern, severity, burn frequency and seasonality, producing contrasting ecological consequences (Steel et al. 2021). Recent years have seen an increase in fire intensity and extension in different regions (Bowman et al. 2020, Pivello et al. 2021), partially attributable to the fact we are experiencing a biosphere temperature that is 1°C above historical records (Masson-Delmotte et al. 2021); it is hypothesized that this intensification could reduce the spatial and temporal variation in fire regimes, called pyrodiversity (Kelly and Brotons 2017), which in turn will generate substantial reductions in biodiversity and ecosystem processes such as carbon storage (Dieleman et al. 2020, Furlaud et al. 2021). The regions most affected are likely the ones in which fire has historically been rare or absent. In regions such as tropical forests (Barlow et al. 2020), extreme fires could trigger extensive biodiversity loss as well as major ecosystems changes such as transitions from forest to savannah or shrublands (Hirota et al. 2011, Fairman et al. 2015).

Fires in the Amazon region were historically rare, due to the ability of old-growth forest to maintain enough

moisture to prevent fire spread, even after prolonged drought periods (Uhl and Kauffman 1990). Human activities, specifically deforestation and resulting land-use changes over the past four decades, have created conditions conducive to more frequent and widespread fires across the basin (Alencar et al. 2011, Aragão et al. 2018, Cardil et al. 2020). Another significant factor contributing to this phenomenon is the predicted increase in droughts due to climatic change. Droughts can interact with deforestation, potentially exacerbating land cover conversion and creating a dangerous positive feedback loop (Barlow et al. 2020). Furthermore, human activities such as secondary vegetation slash-and-burn and cyclical fire-based pasture cleaning can serve as ignition sources for forest fires (Aragão et al. 2018). Despite substantial reductions in deforestation rates until 2018 (Feng et al. 2021), previous deforestation activities may still provide sufficient ignition sources for fires to expand into adjacent forests (Aragão et al. 2018). This process could raise the importance of fires unrelated to deforestation (Aragão et al. 2014).

Different models of fire for the Amazon have been developed to predict regime changes under climate change scenarios. Here, we define a regime change as an abrupt transition in fire patterns across large areas, such as a shift from infrequent scattered fires to more frequent and extensive burning (Kelly et al. 2020). These models can be process-based (Le Page et al. 2017) or statistical (Fonseca et al. 2019), and generally consider land-use change and other human activities, as well as local weather conditions, but they usually neglect the spatial dynamics of fire spread. Statistical fire models take into account mainly environmental factors (Turco et al. 2018), while process-oriented models include more mechanistic details (Thonicke et al. 2010), and a few treat spatial dynamical phenomena (Schertzer et al. 2014). Such spatial dynamics are important because they can provide insights into how local interactions give rise to emergent fire patterns (Pueyo et al. 2010), and potentially change the stability characteristics of the entire dynamical system (Levin and Durret 1996).

Simple models of fire have been used as an example of self-organized criticality (SOC), where systems can self-organize into a state characterized by power-laws in different model outputs. For example, the forest fire model of Drossel and Schwabl (1992) (DSM) was proposed to show SOC in relation to the size distribution of disturbance events (Jensen 1998). Power-laws imply scale invariance, meaning that there is no characteristic scale in the model. Later it was shown that DSM does not exhibit true scale invariance (Grassberger 2002) and that the system needs to be somewhat tuned to observe criticality (Bonachela and Muñoz 2009). These facts decreased its theoretical attractiveness, but the model could still be of high practical relevance. Some modifications of the DSM model have been used to predict fire responses to climate change (Pueyo 2007), and other DSM variants can reproduce features observed in empirical studies (Ratz 1995) such as the power-law distributions of the fire sizes, the size and shape of unburned areas and the relationship between annual

burned area and diversity of ecological stages (Zinck and Grimm 2009). An analysis of different models showed that the key for reproducing all these patterns was changing the scale of grid cells to represent several hectares, and the 'memory effect': flammability increases with the time since the last fire at a given site (Zinck and Grimm 2009, Zinck et al. 2011). However, the exponent of the fire size distribution observed in different ecoregions cannot still be reproduced by these models.

The simple models mentioned above could have critical behaviour characterized by a power-law distribution in fire sizes and other model outputs. Such dynamics can be explained in terms of percolation theory (Stauffer and Aharony 1994) where there is a transition between two states: one where propagation of fires occurs, and another where it is very limited. The narrow region where the transition occurs is the critical point, characterized by an order parameter (fire size) that depends on some external control parameter (e.g. ignition probability) (Solé and Bascompte 2006). An example of this transition could be the case of the recent Australia 2019-2020 mega-fires (Nolan et al. 2020, Nicoletti et al. 2023), which had devastating consequences for biodiversity and ecosystem functioning (Kelly et al. 2020). Historically, indigenous fire stewardship in Australian landscapes maintained flammable forest in a disconnected state by producing frequent small scale fires ("Biodiversity in flames" 2020), thus preventing high-intensity fires and protecting biodiversity. This regime was disrupted by fire suppression related to European colonization land-use change (Hoffman et al. 2021) and climate (Adams et al. 2020), pushing the system toward a critical regime (Nicoletti et al. 2023) with less ecosystem resilience to extreme fires. These extreme events are very difficult to predict by Earth system models that do not fully incorporate the dynamic of fuel accumulation and vegetation dynamics or their effects on biodiversity and ecosystem services (Sanderson and Fisher 2020).

The objective of this work is to model and predict the changes in fire regimes in the Amazon region using a simple spatial stochastic fire model, based on variables like precipitation and temperature that are included in climate change scenarios. Our hypothesis is that climate change could drive Amazonian fire regime near a critical region, leading to more extreme fires. We thus assume that the emergent dynamics can be described by a process of slow accumulation of fuel and rapid discharge produced by the fires. More precisely, we initially reconstruct past fire patterns using the NASA Moderate-Resolution Imaging Spectroradiometer (MODIS) burnt area product. This step serves to verify our main assumption and to derive an ignition probability. Subsequently, in the second step, we predict the ignition probability up to the year 2060 based on different greenhouse gas Representative Concentration Pathways. The third step involves simulations to explore the behavior of the Fire model. In the fourth step, we fit the Fire Model to the observed MODIS fire patterns. Finally, utilizing the model forced with the ignition probability, we predict and analyze potential changes in the modeled fire regimes for the Amazon, taking into account the influence of deforestation on

model parameters.

We will employ a modified DSM forest fire model (Drossel and Schwabl 1992), incorporating elements of long-distance forest dispersal and seasonality. Notably, the methodology involving the prediction of ignition probability under diverse global change scenarios and subsequent application to force the fire model represents a novel approach, as far as we are aware.

Methods

Our study region is the Amazon biome (Figure S1). This includes Brazil, which represents 60% of the area, as well as eight other countries (Bolivia, Colombia, Ecuador, Guyana, Peru, Suriname, Venezuela, and French Guiana). We chose this region because a significant amount of fires extend to tropical moist forests outside Brazil (Cardil et al. 2020), and the whole area is thought to be a crucial tipping element of the Earth-system (Staver et al. 2011, Lenton and Williams 2013).

Reconstruction of past fire patterns from MODIS data

We estimated the monthly burned areas from 2001 to the end of 2021 using the NASA Moderate-Resolution Imaging Spectroradiometer (MODIS) burnt area Collection 6 product MCD64A1 (Giglio et al. 2016), which has a 460 m pixel resolution. We used Google Earth Engine with the JavaScript programming language to download the data restricted to the region of interest (see source code availability below). Each image represents the burned pixels as 1 and the non-burned as 0. We then calculated the burned clusters using four nearest neighbours (Von Neumann neighbourhood) and the Hoshen–Kopelman algorithm (Hoshen and Kopelman 1976). Each cluster contains contiguous pixels burned within a month and this represents a fire event S, allowing us to calculate the number and sizes of fire clusters by month. We estimated the probability of ignition f as $f(t) = \frac{|S_t|}{T}$, where $|S_t|$ denotes the number of clusters S_t that start in the month t (if a fire started in the previous month we avoided it to remove possible double counting), and T is total number of pixels in the region, to allow comparisons with the fire model.

We also estimated the distribution of fire sizes using an annual period to have enough fire clusters to discriminate between different distributions. We aggregated the monthly images using a simple superposition; the annual image has a 1 if it has one or more fires during the year, and 0 if it has none. This assumes that most of the sites burn only once a year, we verified this using the MODIS data that on average only 0.06% burn more than once annually. After that, we ran again the Hoshen–Kopelman algorithm to obtain the annual fire clusters. In this last case, it is probable that independent ignitions merge into a single fire cluster. Similar methodologies allowing the merging of independent fires have been utilized in global

fire studies (Andela et al. 2017). Then we fitted the following distributions to the fire sizes: power-law, power-law with exponential cut-off, log-normal, and exponential. We used maximum likelihood to decide which distribution fit the data best using the Akaike Information Criteria (AIC) (Clauset et al. 2009). Additionally, we computed a likelihood ratio test, Voung's test (Vuong 1989), for non-nested models. We only considered it a true power-law when the value of the AIC was at a minimum and the comparison with the exponential distribution using the Vuong's test was significant with p<0.05; if p>=0.05 we assumed that the two distributions cannot be differentiated.

Fitting of ignition parameter

We calculated the monthly ignition probability f and related it to monthly precipitation (ppt), maximum temperature (T_{max}) and a seasonal term (m). These variables have generally been included in global and regional fire activity models (Huang et al. 2015, Turco et al. 2018, Fonseca et al. 2019, Wei et al. 2020). More variables were used in these models, but we are constrained by the variables available in the Climate Projections (see below). We obtained environmental data from the TerraClimate dataset (Abatzoglou et al. 2018), averaging over the study region, to represent the influence of regional climate over f. We evaluated an increasingly complex series of generalized additive models (GAMs), assuming a Gaussian distribution and transformed f to logarithms, because it had a highly skewed distribution. We also fitted the same models assuming a Gamma distribution and no transformation for f. For all the models we used thin plate regression splines (Pedersen et al. 2019) as smoothing terms, and for interactions between environmental variables we used tensor products, using restricted maximum likelihood (REML) to fit to the data (Pedersen et al. 2019). All these procedures were available in the R package **mgcv** (Wood 2017) and all source code is available in the repository https://.

We selected the best models using AIC (Wood 2017). To evaluate the predictive power of the models, we split the data set into a training set representing 85% of the data and testing set (always 3 years long) and repeated the procedure 10 times starting at different random dates. We then calculated the mean absolute error (MAE) and the Root Mean Squared Error (RMSE) for the three best models selected with AIC (Table S2). The formulas of MAE and RMSE are as follows:

$$\text{MAE} = \frac{1}{n}\sum_{i=1}^{n}|f_i - \hat{f}_i|$$

$$\text{RMSE} = \sqrt{\frac{1}{n}\sum_{i=1}^{n}(f_i - \hat{f}_i)^2}$$

Where f_i is the observed ignition probability f at month i, $\hat{f}_i$ the predicted f and n the total number of months used for predictions. We selected the model with the smallest Mean Absolute Error (MAE)

and Root Mean Square Error (RMSE) to generate predictions of the ignition probability up to 2060. These predictions serve as input for the fire model, as explained in more detail below. Driving data were obtained from the NASA Earth Exchange Global Daily Downscaled Climate Projections NEX-GDPP (https://www.nccs.nasa.gov/services/data-collections/land-based-products/nex-gddp)(Thrasher et al. 2012), which were estimated with General Circulation Models (GCM) runs conducted under the Coupled Model Intercomparison Project Phase 5 (Taylor et al. 2012). We averaged over the 21 CMIP5 models and over the study region to obtain the monthly values of the variables needed: precipitation and maximum temperature. Then we estimated the probability of ignition up to 2060 using the fitted GAM across two of the four Representative Concentration Pathways (RCPs), RCP4.5 and RCP8.5 (Meinshausen et al. 2011). Such RCPs are greenhouse gas concentration trajectories adopted by the IPCC and used for climate modelling and research (Moss et al. 2010). RCP4.5 represents an intermediate scenario, indicating a peak in emissions around 2040 followed by a decline. On the other hand, RCP8.5 depicts a scenario where emissions persistently increase throughout the 21st century.

Fire Model definition and exploration

Conceptually the model represents two key biological processes: forest burning and forest recovery. We assume that the forest layer represents the flammable biomass or fuel layer of the forest (rather than absolute forest cover), as the focus is on modeling fire spread dynamics. When a site is burned in the model, it does not necessarily mean that all vegetation is killed - rather, it represents the consumption of flammable fuels. The regrowth or recovery process simulates vegetation re-establishing flammable biomass over time. The model lacks a spatially explicit representation of the deforestation process. This deliberate simplification was made to maintain model simplicity and ensure a more manageable fitting procedure for the current scope of the research.

The model uses a two-dimensional lattice to represent the spatial region. Each site in the lattice can be in one of three different states: an empty or burned site, a flammable forest (called forest for short), or a burning forest. The lattice is updated in parallel, according to the following steps:

1. We pick at random a burning site, and it becomes an empty site in the following step (the model's timestep is one day)
2. We pick at random a forest site and it becomes a burning forest if one or more of its four nearest neighbour sites are burning
3. We pick at random another forest site and it sends (with probability p) a propagule to an empty site

at a distance drawn from a power-law dispersal kernel with exponent de.

4. A random site can catch fire spontaneously with probability f, i.e., which varies monthly to reflect the fire season. This parameter is fitted to fire data for predictions, global change scenarios, and deforestation scenarios (refer to the previous section for details).

We assumed absorbing boundary conditions and a lattice size of 450x450 sites, but also ran simulations with other sizes, resulting in equivalent results. Rule 3 means that a burned or empty site can become forest more quickly when it is near a forest site, but also that some sites can become forest even when far from established forest sites–depending on the kernel exponent, it could be any site in the lattice (Marco et al. 2011). The choice of a power-law dispersal is justified because forests dispersion generally exhibits fat-tailed kernels (Clark et al. 2005, Seri et al. 2012).

This model is very similar to the DSM forest fire model (Drossel and Schwabl 1992): it exhibits critical behaviour when $\theta = p/f$ tends to ∞, and thus must satisfy the condition that $f << p$. This condition means that the chances of an empty site turning into forest are much higher than the chances of a healthy forest site catching fire spontaneously, as is generally observed in natural systems. The model involves the separation between three time scales: the fast burning of forest clusters, the slow recovery of forest, and the even slower rate of fire ignition. Then in the critical regime there is a slow accumulation of forest that forms connected clusters, and eventually as the ignition probability is very low these clusters connect the whole lattice— here is the link with percolation theory (Stauffer and Aharony 1994)— and a single ignition event can produce large fires. After this, the density of the forest becomes very low and the accumulation cycle begins again. This regime is characterized by wide fluctuations in the size of fires and the density of trees, with both following approximately power-law size distributions. If the ignition probability f is too high fires are frequent, forest sites become disconnected and small fires, of characteristic size, dominate the system.

One of the features not present in the original forest fire model is that forests can have long-distance dispersal; ecologically, this determines population spread, the colonization of empty habitats, and the assembly of local communities (Nathan et al. 2008). The inclusion of long distance dispersal can modify the distribution of forest clusters, the distribution of fire sizes, and the dynamics of the model (Marco et al. 2011). When forest dispersal is limited mainly to nearest neighbours, forest recovery produces clusters that tend to coalesce and form uniform clusters with few or no isolated forest sites. When the forest burns, these isolated forest sites are the points from where the forest recovers (assuming no external colonization); when these are not present there is an increased probability that the forest becomes extinct. With long-distance dispersal, there is an important number of isolated forest sites, thus decreasing the probability of forest extinction (Figures S12 &

S13). These processes are particularly important when θ is low and fires are smaller but more frequent. In dynamical terms there is a critical extinction value θ_{ext}, when $\theta < \theta_{ext}$ the forest become extinct. However, the critical value depends on the dispersal distance governed by d_e. At higher d_e, the dispersal distance is smaller, the forest patches are more compact and isolated, leading to a higher probability of complete burning and a lower θ_{ext}.

The second feature not present in the original forest fire model is seasonality. In natural systems, certain times of the year exhibit environmental conditions that significantly increase the probability of fire ignition, while during the remaining periods, the probability of fires is much lower. This results in a periodic cycle of forest accumulation and a brief duration of intense fires, commonly known as the fire season. Consequently, the model incorporates a short period characterized by a low θ_{min} and a longer period with a high θ_{max}. When both the minimum and maximum θ values fall within the critical region, the model's long-term behavior resembles the critical regime, with maximum fire sizes occurring during the fire season. If θ_{max} is within the critical region and θ_{min} is outside it, the model's dynamics may exhibit more extreme fires (similar to the critical regime) compared to an equivalent non-seasonal model. Conversely, when both θ values are outside the critical region, the dynamics may approach the critical extinction zone. In this scenario, seasonal differences in fire sizes are less pronounced.

Increasing the length of the fire season as predicted in climate change scenarios (Pausas and Keeley 2021) will produce the model to spend more time at a lower θ decreasing the connectivity of the forest and the size of fires. Moreover, this could increase the possibility of critical extinction if both $\theta_{max} and \theta_{min}$ are below θ_{ext}. In this work we assume that the forest is flammable forest; the extinction of this state could mean that environmental conditions become wetter and the forest does not burn anymore. If environmental conditions become drier, the extinction of forest probably means a transition to another type of vegetation and then the conditions to apply this model will no longer hold.

We conducted a set of exploratory simulations, with a range of parameters compatible with what we found for the Amazon region, to characterize the regimes described above (Table S3). Using a lattice size of 450x450 sites, we ran the simulations for 60 years with an initial forest density of 0.3 (we found that different initial conditions gave similar results) and used the final 40 years to estimate the total annual fire size, the maximum cluster fire size, the distribution of fire sizes and the total number of fires. To determine the cluster fire sizes and distributions we used the same methods described previously for the MODIS fire data. We ran a factorial combination of dispersal exponent de and θ and 10 repetitions of each parameter set. First, we ran the experiment with θ fixed, keeping the ignition probability f constant, and then repeated the experiment with seasonality: we simulated a fire season of 3 months each year multiplying f by 10. A

dispersal exponent $de >> 1$ (e.g. $de = 102$) is equivalent to a dispersal to the nearest neighbours, while $de = 2.0155$ corresponds to a mean dispersal distance of 66 sites (Table S3), i.e. long range dispersal.

Fire Model Fitting

As we already estimated the f parameter from the 21 years of MODIS data, we only needed to estimate the dispersal exponent de and the probability p of forest growth. This parameter p is expressed as $r = 1/p$, representing the average number of days for forest to recover. For this estimation we duplicated the extension of the estimated f as if it started in 1980; we allowed 20 years for transient effects to dissipate in the model, and then used the last 20 years to compare with monthly fire data. This choice was justified because most human activities in the Amazon started in this decade during the conversion of large areas of forest to agriculture (Brando et al. 2019).

To explore the parameter space we used Latin-hypercube sampling (Fang et al. 2005) with parameter ranges $2.5 - 2.00035$ for de (equivalent to a mean dispersal distance range of 3 - 290 sites) and $365 - 7300$ days for r. As the model has a long transient period, we could suppose that the system is in a transient state, and thus we also estimated the initial forest density as a parameter with a range of densities of 0.2 - 0.7. We used 600 samples and 10 repeated simulations of the model for each sample, totalling 6000 simulations, and selected the best parameter set using Approximate Bayesian Computation (ABC) (Csilléry et al. 2010, 2012) by comparing the relative monthly fire size — i.e., the absolute size divided by the total number of sites (the number of MODIS pixels for the Amazon basin or the number of lattice sites for simulations) – with model predictions using Euclidean distance. During an initial test, we observed that the peaks in the model were delayed by 2-3 months; the same happens in more realistic process-based models (Thonicke et al. 2010), and as we were not interested in predicting the exact seasonal fire patterns, so instead of using the complete monthly time series we used the monthly maximum fire size of the year. We validated this choice using a random model simulation with known parameters as data and verifying that we could recover the parameters (see source code). The second step of our fitting procedure was to use power-law fire distribution to perform another ABC; we thus ran 10 simulations for each of the parameter sets in the posterior distribution and then calculated the fire cluster distributions using the same methods explained previously. We used ABC to select a second posterior parameter distribution compared to the median value of the power-law exponent from MODIS data. The tolerance (proportion of results accepted nearest the target values) for both ABC procedures was set at 0.05.

Finally, we ran the model with the final posterior parameter distribution, the ignition probability estimated from the MODIS data, and the ignition probability estimated with the GAM model for the period 2000-2021,

to check if the data fit the prediction range. We performed the ABC using a lattice size of 450x450 sites, and as we used relative values (e.g. absolute fire size divided by the total number of sites) the model does not represent a defined scale.

Model Predictions

We used the set of posterior parameter distribution set and the predictions of the parameter f under RCP4.5 and RCP8.5 to perform simulations up to 2060. We started simulations in the year 1980 as in the fitting procedure, but instead of using f derived directly from data, we used f obtained from the GAM model, allowing us to compare actual and predicted fires using the same method to obtain f.

Our model also does not explicitly account for deforestation's impact; however, we approximate this by dynamically adjusting parameters as deforestation intensifies. Initially fitted to the entire region based on a singular flammable forest type assumption, these parameters reflect an average between two vegetation categories: 1) post-deforestation vegetation, featuring higher ignition probability (f) and faster recovery (associated with higher growth probability, p); and 2) the original forest, with lower f and p values. Consequently, escalating deforestation leads to an estimated increase in the average p and f values beyond the fitted period (see supplementary material for more details). Leveraging the Hansen remote sensing product (Hansen et al. 2013) updated until 2021, we calculated the mean deforestation rate for the Amazon biome. Subsequently, under RCP4.5 and RCP8.5 scenarios, we demonstrate the potential impact of deforestation on the model's predictions. The estimated increase in f post-2021 is shown in Figures S19 & S20.

Results

Fire patterns from MODIS data

The monthly fires follow a strong seasonal pattern with a maximum between September and October (Figure S2). We characterize the annual fire regime using the total fire size (total burned area) and the maximum fire cluster (the biggest fire event S_{max}). We note that the years with highest S_{max} are also years with a large total area size (Figure 1). The years 2007 and 2010 had the two highest S_{max} and they also have a power-law distribution (Table S1, Figures S3-S5). Power-law distributions are defined as $cS^{-\alpha}$ where c is constant, α the exponent and have an extra parameters: $S = x_{min}$, which is the minimum value for which the power-law holds. The constant c is given by the normalization requirement (Newman 2005). In the dataset, only 6 out of 20 years demonstrate fire sizes that conform to a power-law distribution (Table S1, Figures S3-S5). It is noteworthy that some of these distributions display a range $[S_{max} - x_{min}]$ with notably higher values compared to years without power-law behavior. However, variability exists, as certain years

with power-law patterns exhibit a relatively small range. This dual extremity mirrors a discernible pattern observed in the fire model under investigation.

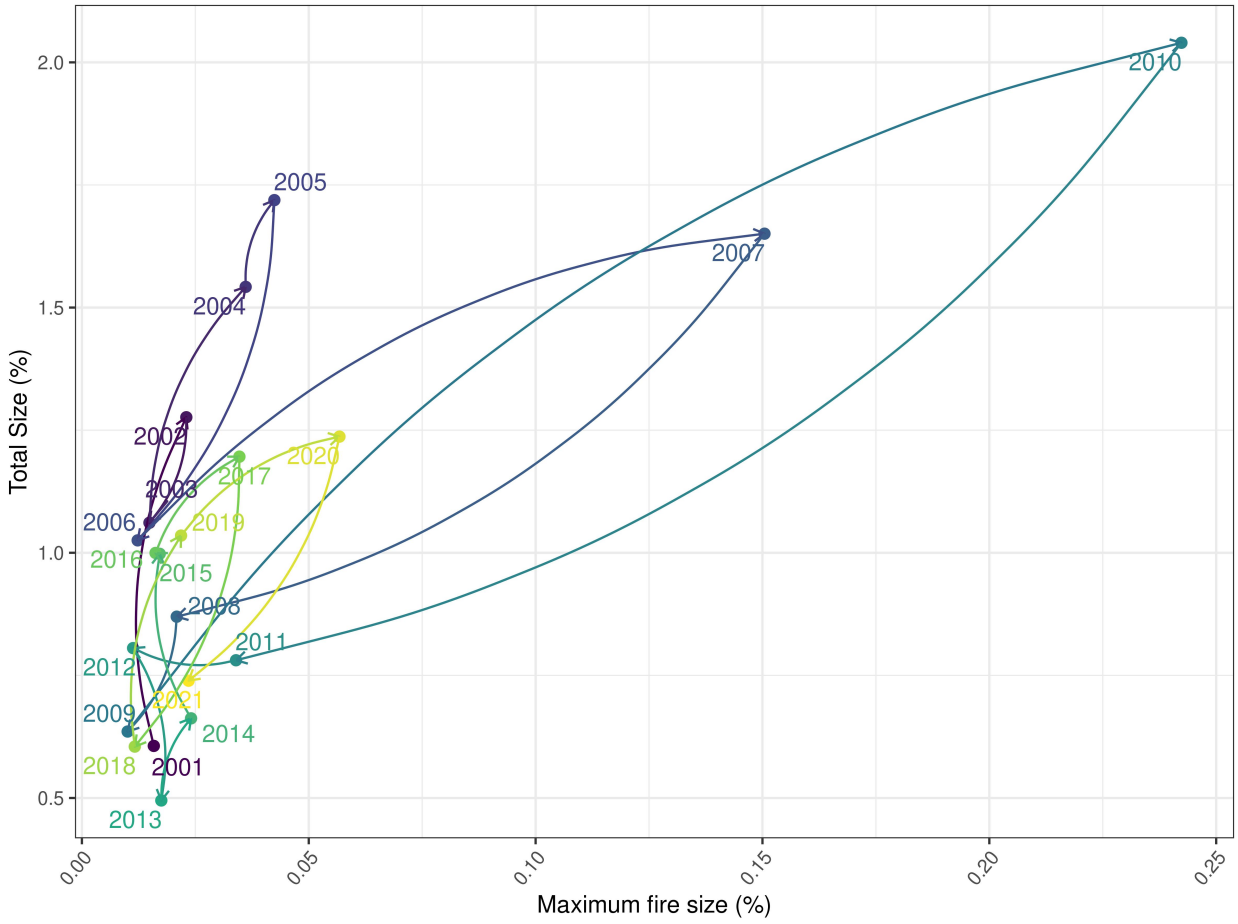

Figure 1: Annual total fire size vs maximum fire size relative to Amazon basin, estimated with MODIS burned area product. These observed data exhibit cycles of loading and discharge, years with high fire extension and big fire events—the upper right region of the figure—which are followed by years of low fire extension and no extreme events in the lower left region. A typical trajectory could be the years 2009, 2010 and 2011 where this cycle can be clearly observed.

Fitting of ignition parameter

We fitted GAM models for the ignition probability f with single variables, combinations of two interacting variables, and lags of one month, the best model with lower AIC and lower MAE and RMSE was the Gaussian with the interaction $T_{max} * m$ (Table S2, Figure S6). For the GAM fitted to the complete dataset we observe that the model does not capture the most extreme years of f (Figure S7), but the model fitted for the first years (< 2018) predicted the rest of the data well (Figure S8).

With the best-fitted GAM and the T_{max} from the NASA Earth Exchange Global Daily Downscaled Climate

Projections, we predicted the monthly f starting from 2021 for two greenhouse gas emissions scenarios: RCP4.5 and RCP8.5. For the fire model simulations we added the GAM's predictions using the actual data previous to 2021, we can observe that the temporal pattern of f before 2021 are seasonal but more irregular and variable than the patterns after 2021 (Figures S9 & S10).

Fire model exploration

We ran the model for a range of the $\theta = p/f$ parameter, anticipating that larger values would produce critical behaviour, consisting of large variability of fires between years and extremely large cluster fire sizes that follow a power-law distribution. As expected, we obtained a larger proportion of power-law distributions for the biggest size of θ (Table S4 & S5), and particularly high variability and extremely large fires (Figure 2). For simulations with seasonality, we observed the expected decrease in the number of years where the size of the fire clusters follows a power-law distribution, also less variability and fewer extreme fires, because in these cases θ decreases for the fire season. Seasonality also had the unexpected effect of increasing the frequency of power-law distribution for $\theta = 25$ with a bigger exponent than the ones for large θ (Table S5); this pattern was also observed in the MODIS data.

In the simulations with $\theta = 25$ and 250 and with shorter dispersal distances, the forest density tends to decrease and eventually reaches zero, marking the absorbing phase transition reported for this type of model (Nicoletti et al. 2023); this means that in these cases the parameter θ was below the critical point θ_{ext} and so produces forest extinction (Figure S11). Increasing the dispersal distance produces higher forest density, while seasonality has the opposite effect. In the case of high dispersal and low θ and seasonality, we are again below θ_{ext} (Figures S12 & S13). Note once again that forest density is the so-called active component of the model and represents the flammable forest.

Fire Model Fitting

After the first ABC we obtained the first posterior distribution of parameters (Table S6). The model generated simulations that closely resemble the monthly MODIS fire estimates, despite being fit only using annual maxima (Figure S14). Repeated simulations with the same set of parameters revealed significant variation due to the stochastic nature of the model dynamics (Figure S14 & S15). A noticeable lag in the model's monthly maxima compared to MODIS data (Figures S14 & S15) may be due to the lack of a fire spread velocity parameter in the model. Despite this, when evaluating the total annual fire size, the model produced intervals that encompassed the MODIS estimates (Figure S16). Thus, the lag in the monthly maxima does not significantly impact our goal of predicting the total annual fire.

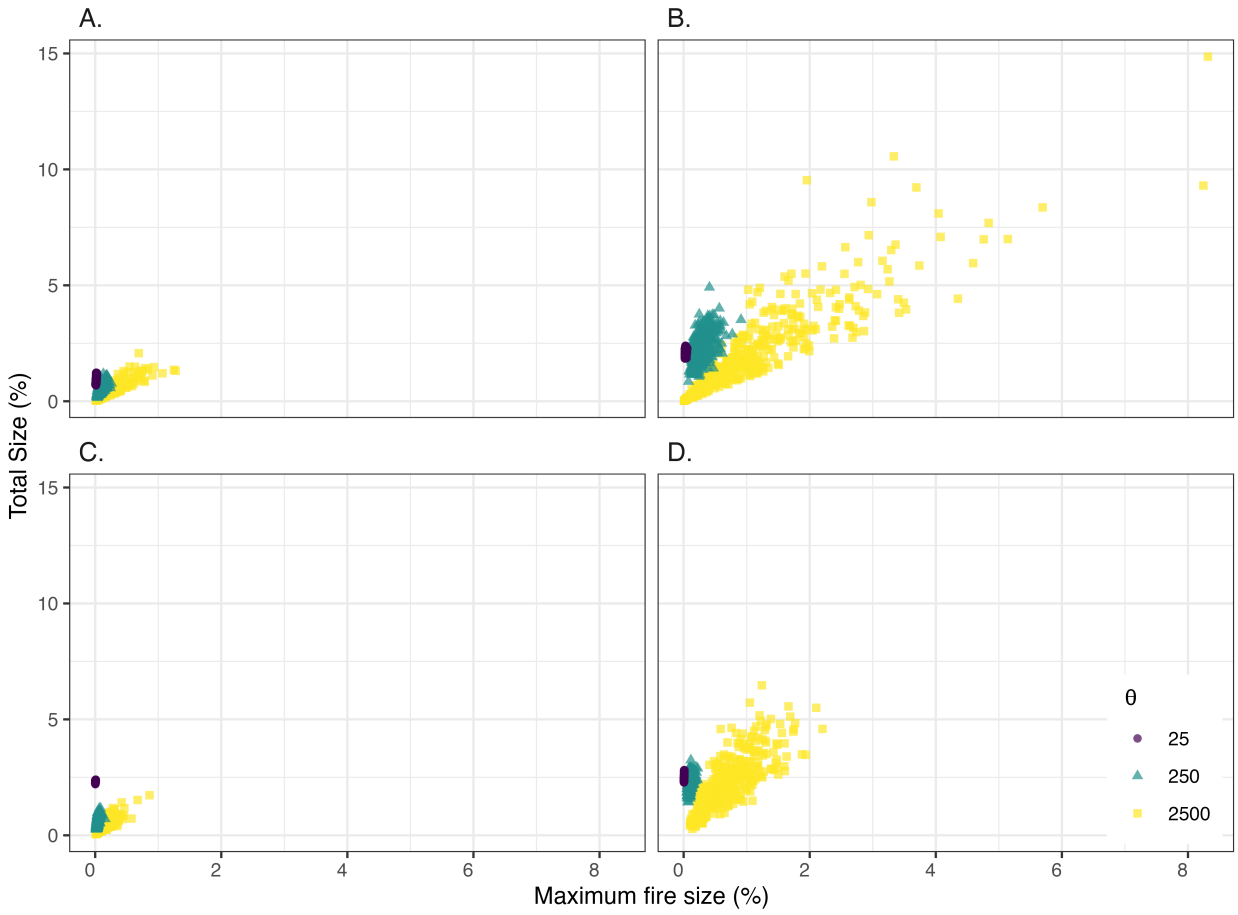

Figure 2: Total annual fire size vs. max fire cluster for the Fire model. **A** & **B** Are simulations with fixed θ, where $\theta = p/f$, p the forest recover probability and f the ignition probability. **A** Are simulations with dispersal exponent $de = 102$, mean dispersal distance of 1 (equivalent to nearest neighbours) and **B** with $de = 2.0155$, mean dispersal distance of 66 sites. **C** & **D** Are simulations with a fire season of 90 days where θ is divided by 10 (the probability of ignition f is multiplied by 10), and the same de as previously.

For the second ABC we used the posterior obtained in the first step, and calculated the power-law exponent of the model simulations; this new set of parameters had a similar range as the first (Table S7), with simulated power-law exponents near the observed value (Figure S17). The average θ of the final posterior distribution has a mean of 61 a range between 9 and 910, which is a low-intermediate range, considering the parameter range we used for the model exploration. The active state of the model, representing the amount of forest, consistently displayed a median value of 0.2 across all scenarios (Figure S18).

When examining predictions without temporal structure (Figure 3), both models, one simulated with the ignition probability (f) calculated from the data and the other with f estimated using the GAM model, produced results consistent with the observed data range. Comparing medians, the predicted total fire size closely matched the data (Figure 3A), while the predicted number of fires was slightly higher (Figure 3C). The maximum fire size (S_{max}) was moderately elevated (Figure 3B), and the power-law exponent (α) of the fire size distribution was lower (Figure 3D). It is worth noting that these results are interconnected, as a lower α signifies larger fire events. The model exhibited an extended range with a few very large fires, an outcome expected due to the nonlinear nature of the model and the number of simulations (around 100 for each observed data).

Fire model predictions

The modelled temporal series, based on the f from the GAM model for the 2001-2021 period, exhibits a 95th percentile interval that encompasses almost all the fire data (with the exception of the 2010 extreme fire). The median of the series suggests a decreasing trend in annual fires over this time period (Figure 4). This decrease, along with inter-annual fluctuations, is also apparent in the observational fire data shown in Figure 1. Specifically, the most extensive fires occurred in the first decade from 2001-2010, while the subsequent period from 2011-2021 experienced substantially less extensive burning. After 2021, the model utilizes General Circulation Model (GCM) predictions to estimate the fire ignition f, and a mean rate of deforestation from data.

Under both RCP scenarios in the absence of deforestation, a consistent pattern emerges with a gradual increase in the total annual fires. However, the annual peak values observed in this scenario remain below those recorded during the 2001-2021 period. In contrast, when considering deforestation, a notable surge is evident in both the median and extreme annual fire occurrences (Figure 4). While both RCP scenarios exhibit comparable trends, there is an expansion in the range of annual fires within the RCP8.5 scenario. This expansion is primarily driven by lower minimum fire occurrences.

The trends depicted in the total annual versus maximum fire plot by decade (Figure 5) align with the obser-

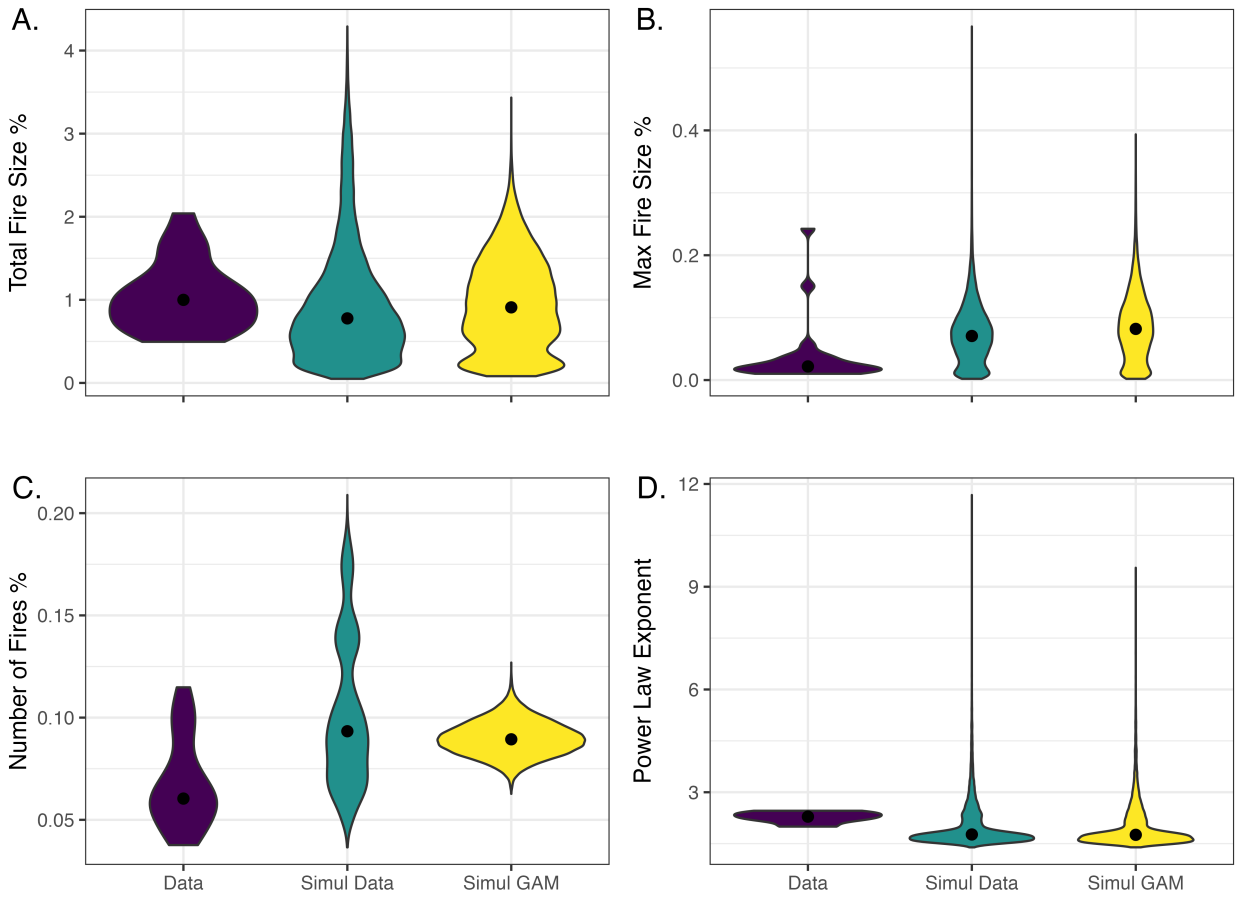

Figure 3: Predictions of the fire model compared with observed data for the years 2001-2021. We used best-fit parameters, the ignition probability from MODIS, and the ignition probability from the estimated GAM models (Simul GAM), and run 100 simulations of the model. To make them comparable we divided all the outputs (except power-law exponent) by the total number of pixels in the region/model; black points are the medians.

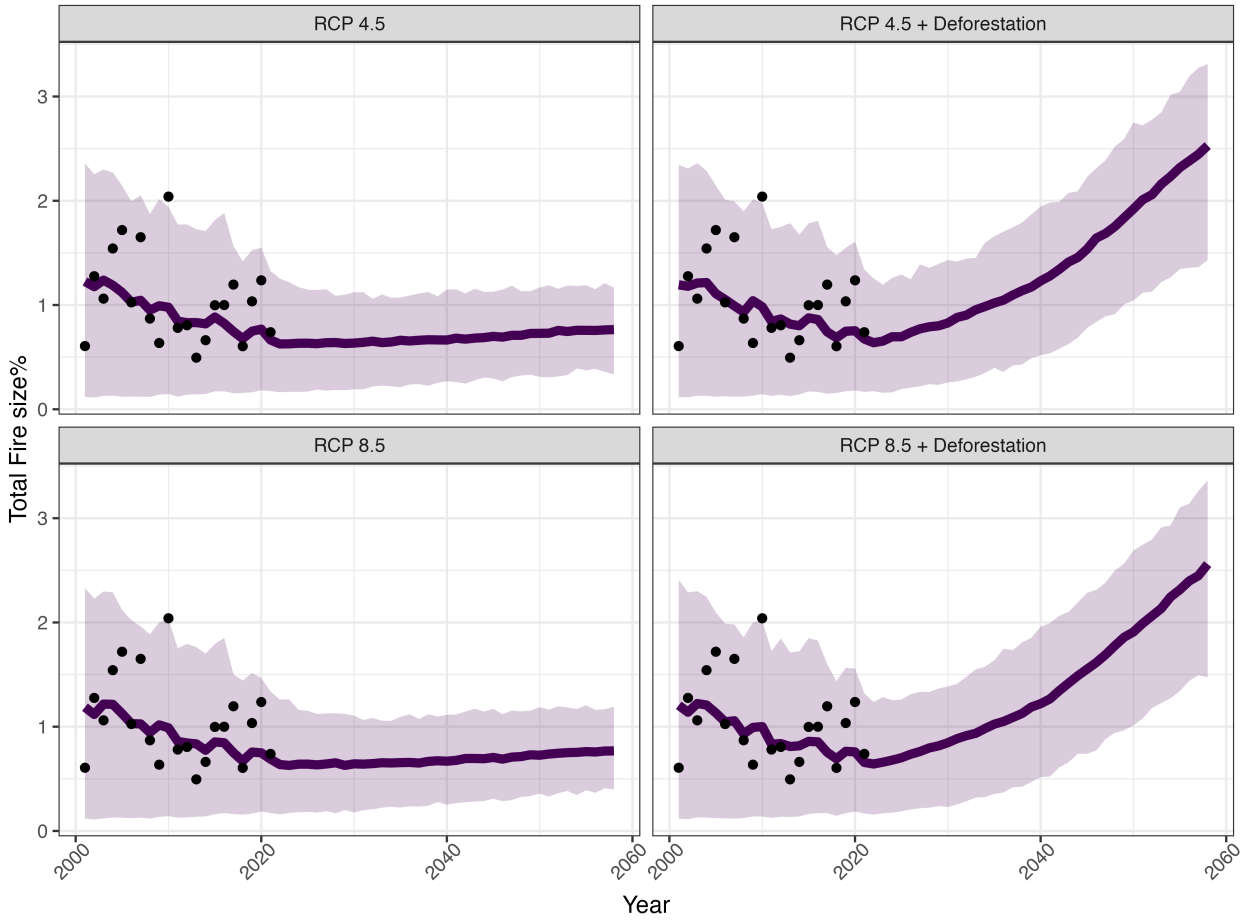

Figure 4: Time series of predictions of the fire model without (left) and with (right) deforestation, compared with observed data for the years 2001-2060. We used best-fit parameters distribution, the ignition probability derived from GAM models estimated using actual data up to 2021, and projections based on General Circulation Models (GCMs) following two greenhouse gas emissions scenarios, namely Representative Concentration Pathways (RCPs) 4.5 and 8.5 for subsequent years. The data points represent actual observations, while the line denotes the median of simulations with accompanying 95% confidence interval bands. All outputs are presented relative to the total area.

vations described above. The plot encompasses all model simulations, highlighting the model's proficiency in simulating extreme fires. However, an anticipated trend solely attributable to climate change scenarios would indicate a decline in extreme fires and total annual fire occurrences. Incorporating deforestation into the analysis revealed a significant escalation in both the maximum fire size and the overall total fire size. Figure 5 illustrates the trend observed for RCP 4.5, which is also similar to that depicted in Figure S21 for RCP 8.5. Both RCP scenarios exhibit a similar pattern.

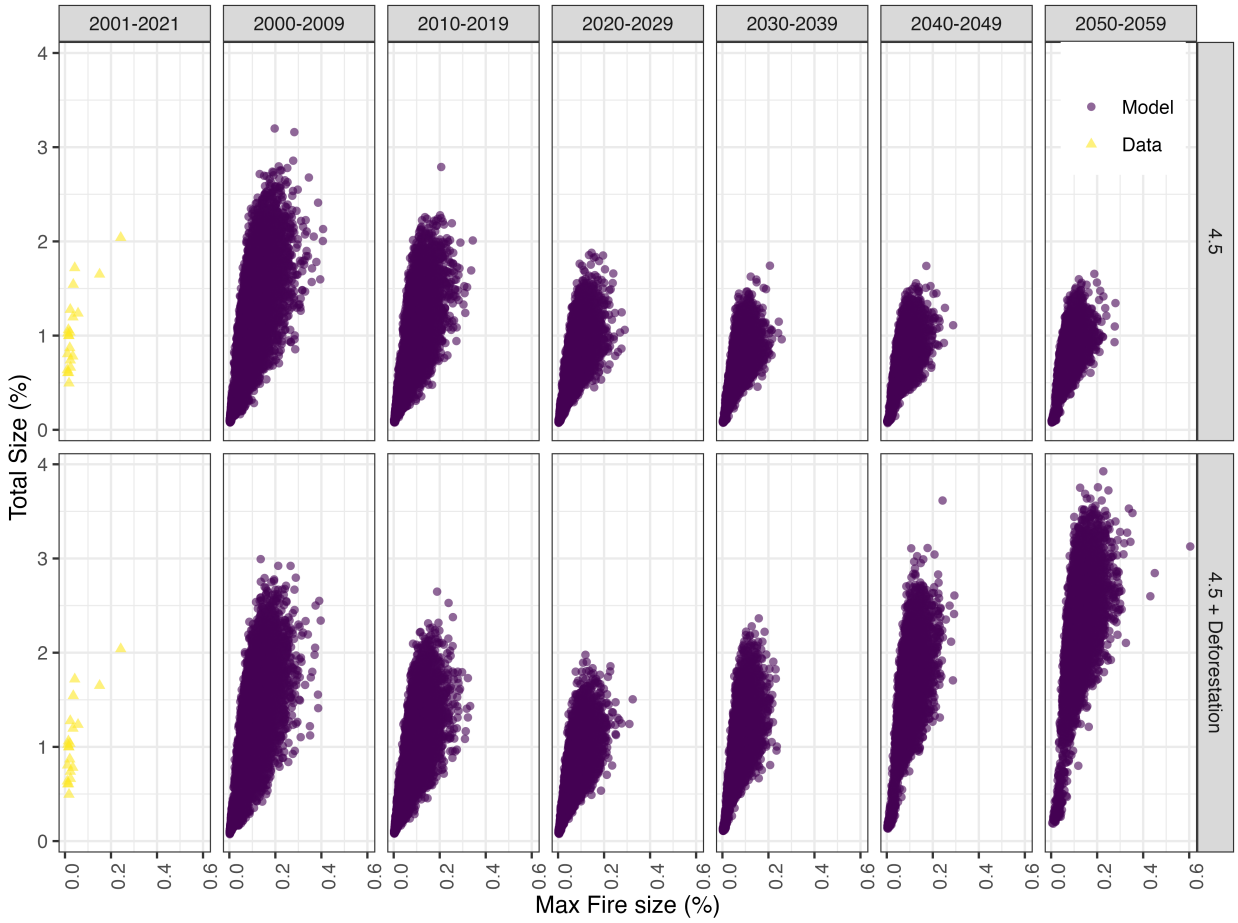

Figure 5: Total annual size of fires vs maximum monthly fire size % relative to the area of the region, data, predictions and predictions including deforestation. The data column was estimated using the MODIS burned area product. The predictions by decade were estimated with a fitted model using a monthly ignition probability calculated with data from General Circulation Models under two greenhouse gas emissions scenarios known as Representative Concentration Pathways (RCPs), here only RCP4.5 and RCP8.5 is shown in the figure S21. For the years 2001-2021 the ignition probability was estimated from actual data.

Discussion

Based on spatial forest-fire dynamics, the model fitted to actual data successfully reproduces past fire patterns and provides insights into the future dynamics of Amazon fires. The predictions up to year 2060 suggest

that the Amazon fire dynamics are driven to an increase in total annual and extreme fires mainly caused by deforestation. Surprisingly, this increase did not occur under a scenario of climatic forcing alone. In fact, in the latter case, the model actually predicts a reduction of extreme annual fires and a slight increase in annual fire size.

This last result might be due to a double average that we used for the General Circulation Models (GCM): we averaged the tempertature over the spatial extension of the region and over all the 21 GCMs. When we used the actual data —also averaged over the region— the model predicts in the range of observed extreme fires. For this reason, we hypothesize that increased temporal variability of the ignition probability could produce an increase in the extreme fires not captured by the model due to the smoothed nature of the CGM data. We furthermore hypothesize that our results might in general underestimate the impact of climate change on total fire size, because our model only assumes increased fire ignition in drier conditions but ignores increased fire propagation under the same conditions.

By contrast, the increase in the median tendency of annual fires under deforestation scenarios appears to be a robust prediction, consistent with the projected rise in fire weather conditions for the region (Abatzoglou et al. 2019). It is furthermore also in line with the observation that declining total fire sizes in years 2001-2021 coincide with decreasing levels of deforestation. The deforestation levels in the Brazilian Amazon were 44% lower in 2020 compared to the levels recorded from 1996 to 2005 (Silva Junior et al. 2020). One interesting application of this model is its ability to provide insights into trends that extend beyond the fluctuations of actual data.

The observed decrease in median total fire size during the period from 2002 to 2021, when the model was fitted to data, could be attributed to the reduction in deforestation levels in the Brazilian Amazon, which were 44% lower in 2020 compared to the levels recorded from 1996 to 2005 (Silva Junior et al. 2020). One interesting application of this model is its ability to provide insights into trends that extend beyond the fluctuations of actual data.

A critical regime would imply far more extreme fires and an absorbing phase transition that could signal an imminent forest-savanna transition, without extreme fires but with more frequent fires. The actual and predicted fire regime seems to lie between these regimes. This model does not explicitly include deforestation or slash-and-burn and other agricultural areas—these are implicitly represented in the flammable forest state—and thus the continuous increase of these land uses represented in the deforestation scenarios, combined with the increase in the probability of ignition f and produce important changes in the Amazonian fire regime.

Similar models have been used to fit fire data and determine if a given system is in a critical regime. For example, Zinck et al. (Zinck et al. 2011) found that some regions of Canada have experienced a change in the fire regime from a non-critical to critical. They argued that the original Drossel-Schwabl model (DSM) did not give the correct values of the power-law exponent of fire distributions, and thus modified the model to represent fire propagation as a stochastic birth-death process. This means modelling fire as a contact process (Oborny et al. 2007) that develops over the forest sites; the same concept was further explored concerning the recent Australian mega-fires (Nicoletti et al. 2023). Here we took a different approach: as in the DSM our model is based on deterministic spread of fire, and we added what we think are the minimal processes needed for more realism: seasonality and forest dispersal distance. We agree with Zink et al. (2011) that an extension of the original DSM was needed to represent fire processes observed in ecosystems, but we also argue that not all complexity can or should be added. In fact, it is necessary to keep the model tractable in order to e.g. perform parameter-space explorations. Our model is consequently phenomenological, in the sense that it does not include all mechanisms present at local scales but still tries to predict fire dynamics at broad scales. Our results identify deforestation as a key driving force for changes in the fire regime. We therefore suggest that future model versions including a deforested state with different ignition f and recovery p probabilities should be built to allow for a rigorous comparision between these types of fire models. Such a comparison clearly goes beyond the scope of the present study but would be needed to gain deeper insights into the role of deforestation.

One of the advantages of this kind of model is that it can be applied to different systems. This is the case for the original DSM model which has been applied to brain activity and rainfalls (Palmieri and Jensen 2020). In these two systems there are cycles of loading and discharge, a broad region where the fluctuations peak as the critical behaviour is established, and not a critical point with a very sharp transition as the theory of second-order phase transitions suggests (Stauffer and Aharony 1994). A similar behaviour occurs in our model version, but not in the original DSM, due to the temporal dependence of the parameters imposed by the fire seasons, where during some months there is a higher ignition probability f. This changes the control parameters with respect to the DMS model since, in fact, we do not observe a transition for a specific value of the θ parameter. Our results suggest that instead of having a specific fine-tuning to observe critical fire spread, a critical region similar to a "Griffiths phase" may be present in our model. Originally defined in statistical physics (Moretti and Muñoz 2013), a Griffiths phase represents an extended region in the parameter space characterized with power-laws scaling behaviour that arises from heterogeneity at local burning patterns. In our model, some areas may experience infrequent small fires as in the historical Amazon, while others see more active, irregular burning influenced by localized factors. However, we lack a

rigorous result in this regard.

We observed the anticipated impact of the 2010 drought on fires in the Amazon biome, resulting in the most extensive fire occurrences on record, even though deforestation rates were significantly lower than in the previous decade (Aragão et al. 2018). In contrast, other drought years, such as the one associated with the El Niño event in 2015-2016, led to a considerably lower number of fires compared to the 2010 drought. This discrepancy may be attributed to the nonlinear loading and discharge cycles inherent in the dynamics of fire-forest systems. Following fires and droughts, fuel accumulates during wetter years, potentially yielding different effects during extreme events. Our model, which incorporates the influence of drought using actual and predicted temperatures to estimate the probability of ignition (f), supports the hypothesis that nonlinear effects play a substantial role in fire dynamics. Using the inverse of the p parameter the model also predicts that the forest will be recovered between 13 and 19 years, close to the 23 years suggested by Alencar (Alencar et al. 2011).

While droughts are considered the primary cause of fires in the Amazon, deforestation is becoming the second (Aragão et al. 2018). In addition, Cardil (2020) found that in 2018 most of the fires (85%) were produced in areas deforested in 2018. The fitted parameters, forced with the ignition probability estimated from actual data are incompatible with such a high proportion, but are close to the proportion observed in previous years. A model incorporating explicit parameters for deforested areas would be needed to resolve this.

The forest state in our model symbolizes flammable forest, given that undisturbed tropical forest in the Amazon is generally considered non-flammable with a very low probability of natural fires (Fonseca et al. 2019). In contrast, deforested areas are flammable, and our fitted parameters encapsulate an average of these scenarios. The proportion of these types is changing due to increased interfaces between undisturbed forest, human-degraded forest, and other land uses (Aragão et al. 2018). Human-induced fires persist, originating from the transportation network and external regions (Barlow et al. 2020). These fires can invade standing forest, and if climate change makes forests hotter and drier, they may sustain more extensive fires (Brando et al. 2019). Our model incorporates these changes by varying the proportion of forest that burns and is deforested. Thus, besides the range of variation in θ is higher for the scenarios with deforestation, but as we maintain the average θ constant at the fitted values, it is also expected that the deforestation scenarios are far from a critical regime as without deforestation. Additionally, as the magnitude of fires increases, the probability of forests losing their capacity to recover from frequent fires and droughts increases (Brando et al. 2019).

Several studies propose that a deforestation rate ranging from 20% to 40% in the Amazon could trigger a swift

transition to non-forest ecosystems (Nobre et al. 2016, Lovejoy and Nobre 2018). Currently, around 20% of the Amazon's forest has been lost since the 1960s, and environmental signals suggest ongoing fluctuations in the system (Lovejoy and Nobre 2018). Analysis of early warning transition signals indicates proximity to a transition point (Saravia et al. 2018). However, our model suggests that the fire regime will not undergo a significant change solely due to climate change; instead, deforestation emerges as the more influential driver. Our primary conclusion is that if deforestation and degradation in the Amazon decrease, the region could exhibit improved resilience against predicted climate change, mitigating the risk of the Amazonian tropical forest collapsing into a savanna. Moreover, asserting the safety of the Amazon solely by halting deforestation is not warranted. Synergies between climate and land use disturbances, as indicated in a recent study by Flores et al. (2024), propose a safe boundary with a cap of 10% accumulated deforestation. Achieving this threshold necessitates extensive restoration efforts to rehabilitate a significant portion of degraded forest.

References

Abatzoglou, J. T. et al. 2018. TerraClimate, a high-resolution global dataset of monthly climate and climatic water balance from 1958–2015. - Scientific Data 5: 170191.

Abatzoglou, J. T. et al. 2019. Global Emergence of Anthropogenic Climate Change in Fire Weather Indices. - Geophysical Research Letters 46: 326–336.

Adams, M. A. et al. 2020. Causes and consequences of Eastern Australia's 2019–20 season of mega-fires: A broader perspective. - Global Change Biology 26: 3756–3758.

Alencar, A. et al. 2011. Temporal variability of forest fires in eastern Amazonia. - Ecological Applications 21: 2397–2412.

Andela, N. et al. 2017. A human-driven decline in global burned area. - Science 356: 1356–1362.

Aragão, L. E. O. C. et al. 2014. Environmental change and the carbon balance of Amazonian forests. - Biological Reviews 89: 913–931.

Aragão, L. E. O. C. et al. 2018. 21st Century drought-related fires counteract the decline of Amazon deforestation carbon emissions. - Nature Communications 9: 536.

Barlow, J. et al. 2020. Clarifying Amazonia's burning crisis. - Global Change Biology 26: 319–321.

2020. Biodiversity in flames. - Nature Ecology & Evolution 4: 171–171.

Bonachela, J. A. and Muñoz, M. A. 2009. Self-organization without conservation: True or just apparent scale-invariance? - Journal of Statistical Mechanics: Theory and Experiment 2009: P09009.

Bowman, D. M. J. S. et al. 2020. Vegetation fires in the Anthropocene. - Nature Reviews Earth & Environment: 1–16.

Brando, P. M. et al. 2019. Droughts, Wildfires, and Forest Carbon Cycling: A Pantropical Synthesis. - Annual Review of Earth and Planetary Sciences 47: 555–581.

Cardil, A. et al. 2020. Recent deforestation drove the spike in Amazonian fires. - Environmental Research Letters 15: 121003.

Clark, C. J. et al. 2005. Comparative seed shadows of bird-, monkey-, and wind-dispersed trees. - Ecology 86: 2684–2694.

Clauset, A. et al. 2009. Power-Law Distributions in Empirical Data. - SIAM Review 51: 661–703.

Csilléry, K. et al. 2010. Approximate Bayesian Computation (ABC) in practice. - Trends in Ecology & Evolution 25: 410–418.

Csilléry, K. et al. 2012. Abc: An R package for approximate Bayesian computation (ABC). - Methods in Ecology and Evolution 3: 475–479.

Dieleman, C. M. et al. 2020. Wildfire combustion and carbon stocks in the southern Canadian boreal forest: Implications for a warming world. - Global Change Biology 26: 6062–6079.

Drossel, B. and Schwabl, F. 1992. Self-organized critical forest-fire model. - Physical Review Letters 69: 1629–1632.

Fairman, T. A. et al. 2015. Too much, too soon? A review of the effects of increasing wildfire frequency on tree mortality and regeneration in temperate eucalypt forests. - International Journal of Wildland Fire 25: 831–848.

Fang, K.-T. et al. 2005. Design and Modeling for Computer Experiments.

Feng, X. et al. 2021. How deregulation, drought and increasing fire impact Amazonian biodiversity. - Nature 597: 516–521.

Flores, B. M. et al. 2024. Critical transitions in the Amazon forest system. - Nature 626: 555–564.

Fonseca, M. G. et al. 2019. Effects of climate and land-use change scenarios on fire probability during the 21st century in the Brazilian Amazon. - Global Change Biology 25: 2931–2946.

Furlaud, J. M. et al. 2021. Bioclimatic drivers of fire severity across the Australian geographical range of giant Eucalyptus forests. - Journal of Ecology 109: 2514–2536.

Giglio, L. et al. 2016. The collection 6 MODIS active fire detection algorithm and fire products. - Remote Sensing of Environment 178: 31–41.

Grassberger, P. 2002. Critical behaviour of the Drossel-Schwabl forest fire model. - New Journal of Physics 4: 17.

Hansen, M. C. et al. 2013. High-Resolution Global Maps of 21st-Century Forest Cover Change. - Science 342: 850–853.

Hirota, M. et al. 2011. Global Resilience of Tropical Forest and Savanna to Critical Transitions. - Science 334: 232–235.

Hoffman, K. M. et al. 2021. Conservation of Earth's biodiversity is embedded in Indigenous fire stewardship. - Proceedings of the National Academy of Sciences in press.

Hoshen, J. and Kopelman, R. 1976. Percolation and cluster distribution. I. Cluster multiple labeling

technique and critical concentration algorithm. - Physical Review B 14: 3438–3445.

Huang, Y. et al. 2015. Sensitivity of global wildfire occurrences to various factors in the context of global change. - Atmospheric Environment 121: 86–92.

Jensen, H. J. 1998. Self-Organized Criticality: Emergent Complex Behavior in Physical and Biological Systems. - Cambridge University Press.

Kelly, L. T. and Brotons, L. 2017. Using fire to promote biodiversity. - Science 355: 1264–1265.

Kelly, L. T. et al. 2020. Fire and biodiversity in the Anthropocene. - Science in press.

Le Page, Y. et al. 2017. Synergy between land use and climate change increases future fire risk in Amazon forests. - Earth System Dynamics 8: 1237–1246.

Lenton, T. M. and Williams, H. T. P. 2013. On the origin of planetary-scale tipping points. - Trends in Ecology & Evolution 28: 380–382.

Levin, S. A. and Durret, R. 1996. From individuals to epidemics. - Philosophical Transactions of the Royal Society of London. Series B 351: 1615–1621.

Lovejoy, T. E. and Nobre, C. 2018. Amazon Tipping Point. - Science Advances 4: eaat2340.

Marco, D. E. et al. 2011. Comparing short and long-distance dispersal: Modelling and field case studies. - Ecography 34: 671–682.

2021. Summary for policymakers. - In: Masson-Delmotte, V. et al. (eds), Climate Change 2021: The Physical Science Basis. Contribution of Working Group I to the Sixth Assessment Report of the Intergovernmental Panel on Climate Change. Cambridge University Press, in press.

Meinshausen, M. et al. 2011. The RCP greenhouse gas concentrations and their extensions from 1765 to 2300. - Climatic Change 109: 213–241.

Moretti, P. and Muñoz, M. A. 2013. Griffiths phases and the stretching of criticality in brain networks. - Nature Communications 4: 2521.

Moss, R. H. et al. 2010. The next generation of scenarios for climate change research and assessment. - Nature 463: 747–756.

Nathan, R. et al. 2008. Mechanisms of long-distance seed dispersal. - Trends in Ecology & Evolution 23: 638–647.

Newman, M. E. J. 2005. Power laws, Pareto distributions and Zipf's law. - Contemporary Physics 46: 323–351.

Nicoletti, G. et al. 2023. The emergence of scale-free fires in Australia. - iScience in press.

Nobre, C. A. et al. 2016. Land-use and climate change risks in the Amazon and the need of a novel sustainable development paradigm. - Proceedings of the National Academy of Sciences 113: 10759–10768.

Nolan, R. H. et al. 2020. Causes and consequences of eastern Australia's 2019–20 season of mega-fires. - Global Change Biology 26: 1039–1041.

Oborny, B. et al. 2007. Survival of species in patchy landscapes: Percolation in space and time. - In: Scaling Biodiversity. Cambridge University Press, pp. 409–440.

Palmieri, L. and Jensen, H. J. 2020. The Forest Fire Model: The Subtleties of Criticality and Scale Invariance. - Frontiers in Physics 8: 257.

Pausas, J. G. and Keeley, J. E. 2021. Wildfires and global change. - Frontiers in Ecology and the Environment 19: 387–395.

Pedersen, E. J. et al. 2019. Hierarchical generalized additive models in ecology: An introduction with mgcv. - PeerJ 7: e6876.

Pivello, V. R. et al. 2021. Understanding Brazil's catastrophic fires: Causes, consequences and policy needed

to prevent future tragedies. - Perspectives in Ecology and Conservation in press.

Pueyo, S. 2007. Self-Organised Criticality and the Response of Wildland Fires to Climate Change. - Climatic Change 82: 131–161.

Pueyo, S. et al. 2010. Testing for criticality in ecosystem dynamics: The case of Amazonian rainforest and savanna fire. - Ecology Letters 13: 793–802.

Ratz, A. 1995. Long-Term Spatial Patterns Created by Fire: A Model Oriented Towards Boreal Forests. - International Journal of Wildland Fire 5: 25–34.

Sanderson, B. M. and Fisher, R. A. 2020. A fiery wake-up call for climate science. - Nature Climate Change 10: 175–177.

Saravia, L. A. et al. 2018. Power laws and critical fragmentation in global forests. - Scientific Reports 8: 17766.

Schertzer, E. et al. 2014. Implications of the spatial dynamics of fire spread for the bistability of savanna and forest. - Journal of Mathematical Biology 70: 329–341.

Seri, E. et al. 2012. Neutral Dynamics and Cluster Statistics in a Tropical Forest. - The American Naturalist 180: E161–E173.

Silva Junior, C. H. L. et al. 2020. The Brazilian Amazon deforestation rate in 2020 is the greatest of the decade. - Nature Ecology & Evolution: 1–2.

Solé, R. V. and Bascompte, J. 2006. Self-organization in Complex Ecosystems. - Princeton University Press.

Stauffer, D. and Aharony, A. 1994. Introduction To Percolation Theory. - Tayor & Francis.

Staver, A. C. et al. 2011. The Global Extent and Determinants of Savanna and Forest as Alternative Biome States. - Science 334: 230–232.

Steel, Z. L. et al. 2021. Quantifying pyrodiversity and its drivers. - Proceedings of the Royal Society B: Biological Sciences 288: 20203202.

Taylor, K. E. et al. 2012. An Overview of CMIP5 and the Experiment Design. - Bulletin of the American Meteorological Society 93: 485–498.

Thonicke, K. et al. 2010. The influence of vegetation, fire spread and fire behaviour on biomass burning and trace gas emissions: Results from a process-based model. - Biogeosciences 7: 1991–2011.

Thrasher, B. et al. 2012. Technical Note: Bias correcting climate model simulated daily temperature extremes with quantile mapping. - Hydrology and Earth System Sciences 16: 3309–3314.

Turco, M. et al. 2018. Skilful forecasting of global fire activity using seasonal climate predictions. - Nature Communications 9: 2718.

Uhl, C. and Kauffman, J. B. 1990. Deforestation, Fire Susceptibility, and Potential Tree Responses to Fire in the Eastern Amazon. - Ecology 71: 437–449.

Vuong, Q. H. 1989. Likelihood Ratio Tests for Model Selection and Non-Nested Hypotheses. - Econometrica 57: 307–333.

Wei, F. et al. 2020. Nonlinear dynamics of fires in Africa over recent decades controlled by precipitation. - Global Change Biology 26: 4495–4505.

Wood, S. N. 2017. Generalized Additive Models: An Introduction with R, Second Edition. - CRC Press.

Zinck, R. D. and Grimm, V. 2009. Unifying wildfire models from ecology and statistical physics. - The American naturalist 174: E170–85.

Zinck, R. D. et al. 2011. Understanding Shifts in Wildfire Regimes as Emergent Threshold Phenomena. - The American Naturalist 178: E149–E161.